21st CIRP Conference on Life Cycle Engineering

Resource-efficient ball screw by adaptive lubrication

J. Fleischer, U. Leberle*, J. Maier, A. Spohrer

Karlsruhe Institute of Technology (KIT), wbk, Institute of Production Science, Kaiserstr. 12, 76131 Karlsruhe, Germany

* Corresponding author. Tel.: +49-721-608-47419; fax: +49-721-608-45005. *E-mail address:* Urs.Leberle@kit.edu

Abstract

In this paper, the development of a methodology for reducing the energy demand and increasing the life time of ball screws by minimizing the friction torque with adaptive lubrication of the ball screw nut is presented.

Therefore, a simulation model of the feed axis has been developed and fitted metrologically at an especially designed test stand with an adaptive lubrication system for the ball screw nut. The model allows the calculation of the optimum friction torque of the feed axis and thus determines the need for lubricants in case a deviation to the measured friction torque of the feed axis should arise.

The comparison of tests dealing with the life time of ball screws with standard lubrication and new adaptive lubrication aims at proving the increase of the life time. This endeavor will result in characteristic lubrication strategies for a resource-efficient operation of ball screws during constant operating conditions.

1. Introduction

In feed axis technology, ball screws are a widespread element for transforming rotary motion into translatory motion. During this transformation, a friction torque arises that acts against the applied drive torque. The amount of friction torque has a clear influence on the life time of the ball screws and is significantly depending on lubrication, revolution, temperature and load.

In practice, grease lubricated nuts of the ball screws are often supplied with a greater quantity of lubricant than actually necessary. This is done in order to keep the re-lubrication intervals low. This oversupply of lubricant results in an increase of the friction torque. But also an undersupply of lubricant leads to an increase of the friction torque and consequently to early failure.

Nomenclature

C	Dynamic load rating
F	Force
F_R	Friction force
M_R	Friction torque
P	Lead
Q	Contact load
Z	Number of rolling elements
a	Long semi axis of the contact surface
b	Short semi axis of the contact surface
n	Revolution
p_0	Average surface pressure
r	Radius
v	Velocity
α	Pressure angle
β	Lead angle
κ	Damping coefficient (bearing material)

η	Hertzian coefficient
μ	Friction coefficient
υ	Kinematic viscosity
ξ	Hertzian coefficient
Φ_{FS}	Correction factor
ω	Angular velocity

The objective of the project is to develop a method for reducing energy requirement and increasing the life time of ball screws by minimizing the friction torque using adaptive lubrication.

The ideal friction torque of the feed axis should be calculated by using a simulation model and should be compared to the torque measured via the motor current at the drive of the feed axis. The resulting deviation determines the demand of lubricant which is then applied in appropriate quantity by a mechatronic dosing unit.

2. Simulation model of the feed axis

The simulation model is based on a model of a feed axis which was developed in preliminary work [1]. The model allowed the simulation of the drive torque depending on the position, the load force and the velocity but did not consider the friction torque of the ball screw (Figure 1).

The core of the new model is an extension for considering the ball screw friction torque $M_{R,KGT}$. Together with the bearing friction torque $M_{R,L}$ and the friction force in the guides $F_{R,F}$, it creates the basis for determining the total friction torque of the feed axis $M_{R,G}$ depending on the load force F_a, the feed rate v_a and the temperature of the bearings T_L and of the ball screw nut T_{KGT} (Figure 2).
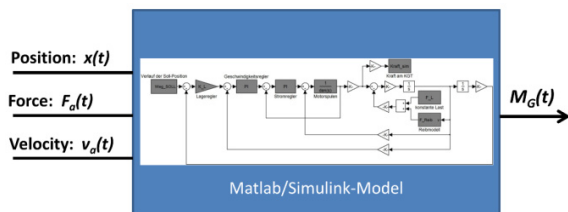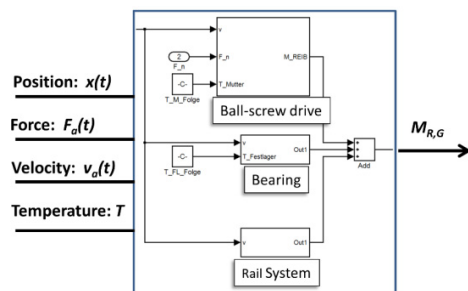

Figure 1: Simulation model of the feed axis

Figure 2: Friction model of the feed axis

Accordingly, the following applies for the total friction torque $M_{R,G}$ of the feed axis:

$$M_{R,G} = \frac{P}{2\pi} F_{R,F} + M_{R,L} + M_{R,KGT} \qquad (1)$$

2.1. Friction model of the ball screw

The friction torque in ball screws to be overcome is made up of several components. Here, the calculations are performed according to the theory for calculating the friction torque in angular contact ball bearings by Baly [2]. This model is adapted to the load situation and the particular kinematics of a ball screw.

2.1.1 Tribology in a rolling contact

The friction torque in rolling contact bearings $M_{R,WL}$ is divided according to Baly [2] into an irreversible deformation work $M_{R,IV}$, a hydrodynamic rolling friction $M_{R,HR}$ and the drilling motion friction $M_{R,BR}$.

$$M_{R,WL} = M_{R,IV} + M_{R,HR} + M_{R,BR} \qquad (2)$$

2.1.1.1. Irreversible deformation work

During the rolling motion, energy has to be applied for compressing the contact surface which is only partly regained when decompressing due to material damping.

The torque from the irreversible deformation work per contact is calculated based on the contact load Q, the contact width in the direction of rolling b and the damping constant of the bearing material κ. Together with the number of balls Z, the angular velocity of the rolling body ω_{WK} and the angular velocity of the internal ring ω_i, the total torque contribution $M_{R,IV}$ is calculated from the irreversible deformation work.

$$M_{R,IV} = Z \frac{\omega_{WK}}{\omega_i} \frac{3}{16} \kappa \sum_{i=1}^{4} b_i Q_i \qquad (3)$$

2.1.1.2. Hydrodynamic rolling friction

The contribution of the hydrodynamic rolling friction goes back to the elastohydrodynamic film of lubricant in the contact point. The overall friction torque $M_{R,HR}$ is calculated from the number of balls Z, the angular velocity of the rolling bodies ω_{WK} and the angular velocity of the internal ring ω_i and the hydrodynamic rolling friction torque with regard to the rotation axis of one ball. The latter results from the diameter of the rolling body r_{WK}, the inner or outer friction forces acting upon the rolling body and a correction value Φ_{FS} introduced by Baly [2] in order to convert the calculated friction force for full lubrication with oil to the one for grease lubrication. The friction forces are hereby calculated with the help of the elastohydrodynamic friction coefficient μ_{EHD} developed by Gohar [4] and the normal forces Q acting in the contact points.

$$M_{R,HR} = Z \frac{\omega_{WK}}{\omega_i} r_{WK} \Phi_{FS} \sum_{i=1}^{4} \mu_{EHD_i} Q_i \tag{4}$$

2.1.1.3. Drilling motion friction

The contribution to the friction torque that is coming from the drilling motion friction $M_{R,BR}$ originates from a drilling motion of the rolling body in the point of contact. A simplified calculation approach was developed by Walter Wernitz [3]. This approach is valid for a drilling motion friction without circumferential slip. In this case, the drilling motion friction torque rotates around the center of the contact area and consists of the transmitted friction force and the corresponding lever arm to the contact center. Integration throughout the whole contact surface then results in the drilling motion friction torque for the contact point. It is calculated from the number of balls Z, the angular velocity of the inner ring ω_i and the drilling motion friction coefficient μ_B and other contact point-specific parameters. These include the angular velocity of drilling motion ω_B, the coefficients ξ and η according to Hertz and the contact point dimensions a and b as well as the maximum pressure p_0 in the contact point.

$$M_{R,BR} = Z \frac{1}{\omega_i} \frac{\pi^2}{8} \mu_B \sum_{i=1}^{4} \omega_{B_i} \xi_i \eta_i^2 a_i^2 b_i p_{0_i} \tag{5}$$

2.1.2. Kinematics in the ball screw

The kinematics of the ball screw requires an adaptation of the friction model that has been developed for the angular contact ball bearing. The reason for this is the lead angle β of the ball screw. This angle leads to a higher circumferential speed v_{GS} (Figure 3, left) and thus, also to higher angular velocities for rolling and drilling motion. Additionally, the ball screw friction torque $M_{R,KGT}$ has to be calculated using an angular function from the friction torque of the bearing $M_{R,WL}$ (Figure 3, right).

Moreover, unstressed preloaded ball screw nuts possess a 4-point contact in the rolling contact which transforms into a 2-point contact at a certain axis load F_a due to the compression in the contact point. At the same time, the rotation axis of the rolling body changes. It is then no longer parallel to the rotating axis of the ball screw but, ideally, parallel to the two contact surfaces.
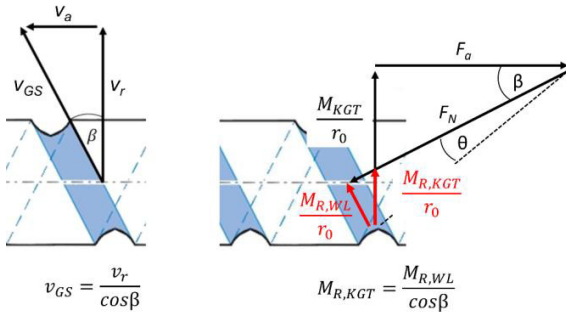
Consequently, the rolling body is not rolling on the effective radius r_{eff} anymore, but on the complete radius of the rolling body r_{WK} (Figure 4). This results in angular velocities of the rolling body ω_{WK} in dependence of the numbers of contacts for a ball screw according to the formulas of Figure 4.

2.1.2.1. Angular velocity during drilling motion

In case of a 4-point contact, the rotating axis of the rolling bodies is parallel to the ball screw axis and offset by the contact angle relative to the contact surfaces (Figure 5, left). However, the 2-point contact's rotation axis of the rolling body ideally lies parallel to the contact surfaces causing a lower angular velocity during drilling motion ω_B (Figure 5, right).

Figure 5 shows the angular velocities of the rolling bodies ω_{WK}, the screw ω'_{GS} and the nut ω'_{GM} in relation to the ball centers. In case of the 4-point contact, the angular velocities in the contact points can be divided into a part that is perpendicular to the contact surface, the angular velocity during drilling motion ω_B, and a part that is parallel to the contact surface, the angular velocity during rolling ω_W. The resulting angular velocities for drilling motion $\omega_{B,i}$ or $\omega_{B,a}$ are thus in compliance with the difference of the two angular velocities for drilling motion ω_B of the contact partners (Figure 5, left). In the 2-point contact, the movement of the rolling body occurs in a way that the rolling body is optimally guided at one contact point. Accordingly, there is no drilling motion at this point. Where the rolling body is guided and where the drilling motion is happening depends on the lubrication and the contact conditions [5].
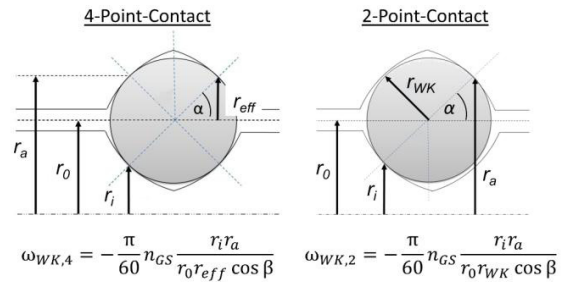

$$\omega_{WK,4} = -\frac{\pi}{60} n_{GS} \frac{r_i r_a}{r_0 r_{eff} \cos \beta} \qquad \omega_{WK,2} = -\frac{\pi}{60} n_{GS} \frac{r_i r_a}{r_0 r_{WK} \cos \beta}$$

Figure 4: Contact situation in the ball screw

$$v_{GS} = \frac{v_r}{\cos\beta} \qquad\qquad M_{R,KGT} = \frac{M_{R,WL}}{\cos\beta}$$

Figure 3: Kinematics in the ball screw

$$\omega_{B,a,4} = (\omega'_{GM} - \omega_{WK}) \sin \alpha \qquad \omega_{B,i,2} = (\omega'_{GM} - \omega'_{GS}) \sin \alpha$$
$$\omega_{B,i,4} = (\omega'_{GS} - \omega_{WK}) \sin \alpha \qquad \omega_{B,a,2} = (\omega'_{GS} - \omega'_{GM}) \sin \alpha$$
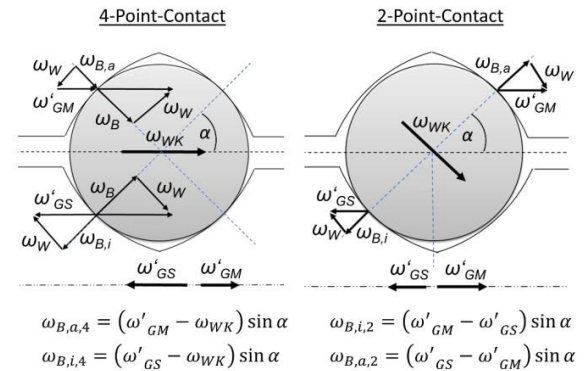
Figure 5: Drilling motion friction in the ball screw

Depending on the point where the guiding occurs, the angular velocities for drilling motion $\omega_{B,i}$ or $\omega_{B,a}$ emerge according to Figure 5, left.

2.1.3. Contact load in the ball screw

The axial force F_a which arises during operation furthermore increases the contact load on two of the four contact points and reduces it on two of them. The contact load reduction stems from the additional deformation of the loaded contact points. This leads to the operating pressure angle $\alpha \neq \alpha_n$ deviating from the nominal pressure angle α_n in unloaded condition. If the axial force exceeds a certain figure, the contact points that have experienced the contact load reduction separate and a two point contact arises.

In a ball screw that is experiencing an axial force F_a, the contact load Q_B arises in the contact point with the additional load and the contact load Q_E declines with the additional unload, depending on the pre-load force F_V (formula 6 and 7).

$$Q_B = \frac{1}{Z \cos \beta} \left(\frac{F_V}{\sin \alpha_n} + \frac{F_a}{\sin \alpha} \right) \tag{6}$$

$$Q_E = \frac{1}{Z \cos \beta} \left(2 \left(\frac{F_V}{\sin \alpha_n} \right)^{\frac{2}{3}} - \left(\frac{F_V}{\sin \alpha_n} + \frac{F_a}{\sin \alpha} \right)^{\frac{2}{3}} \right)^{\frac{2}{3}} \tag{7}$$

2.2. Friction in bearings and guides

Since the here examined relatively low velocities of the feed axis do not lead to any significant warming up of the guides, and since there are no further acting forces besides the weight of the carriage, the guiding friction F_R is assumed to be depending exclusively on the revolution of the ball screw.

Most of the bearing friction is to be attributed to the spindle bearing's fixed bearing. Since the fixed bearing creates a large friction portion of the feed axis' total friction torque, the dependency on revolution as well as temperature need to be considered. However, because of the high preload, a performance independent of the load is assumed for simplification purposes.

2.3. Overall model of the feed axis

The model of the feed axis that has been developed in Matlab Simulink allows the simulation of the total friction torque $M_G(t)$ that needs to be produced by the drive motor, depending on the position, the load and the velocity. Furthermore, it provides the opportunity for calculating the different friction elements of the guides $F_{R,F}(t)$, the bearings $M_{R,L}(t)$ and the ball screw $M_{R,KGT}(t)$.

In the model, the mechanics of the feed axis are considered to be ideal. For illustrating the mechanics, only the mass moment of inertia of the engine shaft and the friction models are reproduced in the model. For further simplification

purposes, the reverse voltage induced by velocity is not fed back since it is negligible for low velocities [4].

The target value signal is calculated by a target position course corresponding to actual movement blocks of feed axis. Furthermore, a load torque is preset as a constant value. It results from the load on the feed axis. The positioning controller is modeled as a P-controller with an amplification factor and the velocity controller is mapped as a PI-controller. The axis' current controller is also described by a PI-controller. The driving motor is modelled as a PT1-element with an electric coil resistance and as a parameter with the coil inductance.

3. Fitting of the simulation model

A special test stand has been set up at the institute for fitting the simulation model. It consists of two parallel feed axes. Their carriages are connected by tension and pressure rods. One of the drives, the positioning drive, is operated in a position-controlled manner. It is at this feed axis, that the previously developed friction model is to be fit.

The operating load F_a is created by the other feed axis in a torque-controlled manner and applied on the carriage of the positioning drive by the tension and pressure rods. The operating load acting on the position-controlled feed axis can be measured by strain gauges located on the tension and pressure rods and it can be adjusted by a suitable adaptation of the target torque of the torque-controlled feed axis.

3.1. Ball screw friction torque determination at the test stand

At the test stand, the total torque of the feed axis $M_G(t)$ corresponds to the motor current of the drive. The friction torque $M_{R,KGT}(t)$ of the ball screw, however, cannot be measured directly. It can only be determined indirectly via the motor current (Figure 6). Therefore, the friction forces in the guides $F_{R,F}(t)$ and in the bearings $M_{R,L}(t)$ of the feed axis need to be determined first.
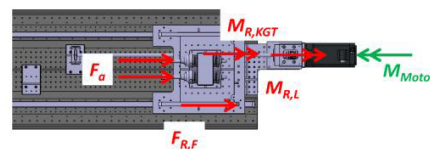
$$M_{R,KGT}(t) = M_G(t) - \frac{5}{2\pi} F_a(t) - \frac{5}{2\pi} F_{R,F}(t) - M_{R,L}(t)$$

Figure 6: Acting forces at the feed axis of the test stand

3.1.1. Friction in guides and bearings

Figure 7 shows the guiding friction measured at the feed axis. The torque $M_{R,F}$ resulting from the guiding friction and acting at the feed axis has been described in equation 8 by a non-linear regression in dependence of the revolution n. For the revolution range over 200 1/min a deviation of maximally 0,01 Nm occurs.

$$M_{R,F} = 5,484 \cdot 10^{-5} n^{0,8} + 0,0606 \qquad (8)$$

Figure 8 depicts the friction in the bearings of the ball screw and the driving motor $M_{R,L}(t)$ in relation to the bearing temperature T_L and the revolution n.

The bearing friction may be described by a non-linear regression (equation 9).

$$M_{R,L} = k_i \left(2,168 n^{0,194} T_L^{-0,42} + 2,823 \cdot 10^{-4} \right) \qquad (9)$$
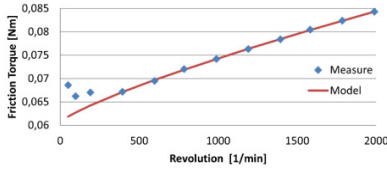

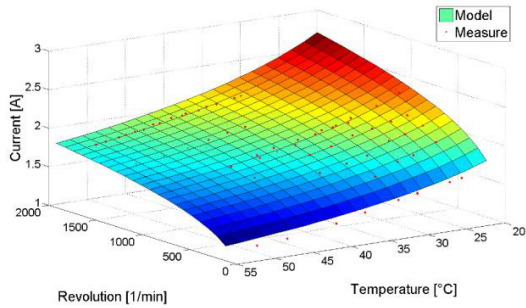Figure 7: Guiding friction for the feed axis

Figure 8: Bearing friction of the feed axis

3.2. Adaptation of the ball screw friction model

The friction model for the ball screw has been adapted according to the data collected at the test stand. A possible deviation of the dependency of the revolution and the temperature is compensated by the correction factor Φ_{FS}. A deviation of the axial force dependency as well as further possible constant deviation components are taken into account by the correction torque M_K.

In consideration of the ball screw lead β (Figure 3), the ball screw friction torque $M_{R,KGT}$ results and consequently the equations 10-15 as well.

$$M_{R,KGT} = \frac{1}{\cos\beta} \left(M_{R,IV} + M_{R,HR} + M_{R,BR} \right) + M_K \qquad (10)$$

$$M_{R,IV} = Z \frac{\omega_{WK}}{\omega_i} \frac{3}{16} \kappa \sum_{i=1}^{4} b_i Q_i \qquad (11)$$

$$M_{R,HR} = Z \frac{\omega_{WK}}{\omega_i} r_{wk} \Phi_{FS} \sum_{i=1}^{4} \mu_{EHD_i} Q_i \qquad (12)$$

$$M_{R,BR} = Z \frac{1}{\omega_i} \frac{\pi^2}{8} \mu_B \sum_{i=1}^{4} \omega_{B_i} \xi_i \eta_i^2 a_i^2 b_i p_{0_i} \qquad (13)$$

Here, the correction factors have been collected by a regression analysis of measuring data of operating forces of $-6000 < F_a < 8000$ N and revolutions of $1400 < n < 2000$ per minute as well as a ball screw nut temperature of $T_{KGT} = 40°C$ and a bearing temperature of $T_L = 45°C$.

$$\Phi_{FS} = \frac{-0,028}{e^{1,48 \cdot 10^{-3} \frac{v}{v_{40}} n}} \qquad (14)$$

$$M_K = 2,54 \cdot 10^{-5} F_a + 0,66 \qquad (15)$$

In particular, the large constant part of the correction torque allows concluding a great deal of overflow lubrication at the moment of measurement.

3.3. Validation of the overall model of the feed axis

The adaptation of the ball screw friction model is followed by a validation of the overall simulation model of the feed axis.

The simulation model is now compared exemplary with the measurements for an axial force of $F_a = 8000$ N and a revolution of $n = 1500$ per minute as well as a ball screw temperature of $T_{KGT} = 40°C$ and a bearing temperature of $T_L = 45°C$.

Figure 9 compares the torques measured at the drive via the motor current and the ones of the simulated overall torque $M_G(t)$ of the feed axis.

The simulated torque corresponds to the measuring data during the acceleration and deceleration process. This indicates a correct mass moment of inertia. However, the oscillating behavior cannot be shown since the mechanics of the test stand were considered to be rigid in the model.

Figure 11 illustrates the simulated ball screw friction torque $M_{R,KGT}(t)$ and the one calculated from the motor current. Here again, the model corresponds well to the ball screw friction torque calculated from the motor current of the feed axis.

As part of the presently conducted permanent tests, Figure 11 demonstrates that the medium ball screw friction torque $M_{R,KGT}$ has continuously decreased during the duration of the tests. After 49,900 cycles, the friction torque has diminished from 0.83 Nm at the moment of the fitting of the model by 50% to 0.4 Nm. During further operation, it is expected that the torque will continue to decrease for quite some time and that it will finally settle at a constant value before it will increase again, due to the prevailing lack of lubricant. Another model adaptation will then be performed for the constant

state. Here, the correction torque M_K will be significantly lower according to equation 15.

Based on this model, the feed axis' optimum friction torque shall finally be calculated in dependence of the operating parameter and shall be compared to the torque measured at the drive of the axis with the motor current.
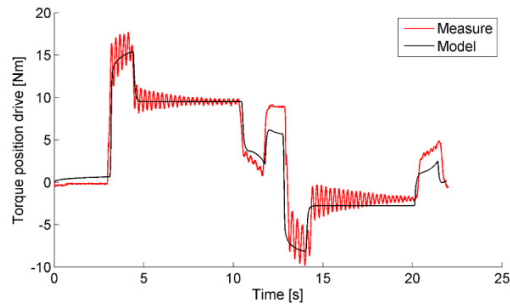

Figure 9: Overall torque $M_G(t)$ simulated and measured via the motor current at F_a = 8 kN and n = 1500 1/min

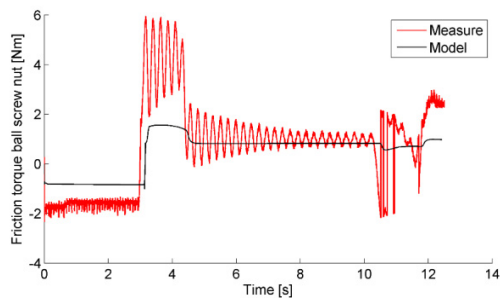Figure 10: Friction torque $M_{R,KGT}(t)$ of the feed axis simulated and calculated from the motor current at F_a = 8 kN and n = 1500 1/min
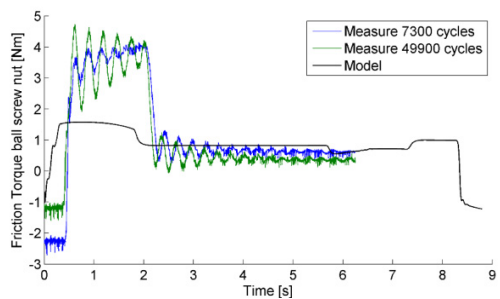

Figure 11: Friction torque $M_{R,KGT}(t)$ of the feed axis (F_a = 8 kN and n = 2000 1/min) simulated and calculated from the motor current at 7,300 and 49,900 cycles

The resulting deviation determines the amount of lubricant that will then be applied in the respective quantity via a lubrication dosing unit.

4. Summary and outlook

The objective of the work at the wbk is the elaboration of a methodology for reducing the energy demand and increasing the life time of ball screws by minimizing the friction torque with adaptive lubrication.

For this purpose, a simulation model of the feed axis has been developed. It allows simulating the acting torque of specific ball screw systems for different points of operation and under consideration of various influencing variables. Afterwards, the model is fitted with measurement at the test stand.

Tests comparing the life time aim at proving the influence of targeted lubrication on the life times of ball screws in the further course of the project. A total of 16 ball screws in industrial standard sizes of 32x5 und 40x20 are going to be analyzed as part of the examinations.

The result shall constitute in characteristic lubrication strategies for a resource-efficient operation of ball screws at constant operating conditions. On one hand, resource efficiency refers to the increase of the life times of the ball screws and on the other hand it refers to the reduction of the energy demand by a minimized friction torque.

References

[1] Hennrich, H., Fleischer, F. Increase of maintenance efficiency by a hybrid diagnosis and prognosis approach. 10th International Conference and Exhibition on Laser Metrology, Machine Tool, CMM & Robotic Performance, Euspen, Bedfordshire, 2013, S. 19-27.
[2] Baly, H. Reibung fettgeschmierter Wälzlager: Wälzlagerreibung Fettschmierung. Hannover: Universität Hannover, 2004.
[3] Wernitz, W. Wälz-Bohrreibung: Bestimmung der Bohrmomente und Umfangskräfte bei Hertz'scher Pressung mit Punktberührung. Braunschweig, Vieweg Verlag, 1958.
[4] Gohar, R. Elastohydrodynamics, New York, World Scientific, 1988.
[5] Eschman, P., Weigand, K. Wälzlagerpraxis: Handbuch für die Berechnung und Gestaltung von Lagerungen. München, R. Oldenburg, 1987.